energies

MDPI

Article

Analyzing the Fast-Charging Potential for Electric Vehicles with Local Photovoltaic Power Production in French Suburban Highway Network

Abood Mourad [1,*], Martin Hennebel [1], Ahmed Amrani [2] and Amira Ben Hamida [2]

[1] Laboratoire Génie Electrique et Electronique de Paris, CentraleSupélec, Université Paris-Saclay, 91190 Gif-sur-Yvette, France; martin.hennebel@centralesupelec.fr

[2] Institut de Recherche Technologique SystemX, 91120 Palaiseau, France; ahmed.amrani@irt-systemx.fr (A.A.); amira.benhamida@irt-systemx.fr (A.B.H.)

* Correspondence: mouradabood90@gmail.com

Abstract: The need for deploying fast-charging stations for electric vehicles (EVs) is becoming essential in recent years. This need is justified by the increasing charging demand and supported by new charging technologies making EV chargers more efficient. In this paper, we provide a survey on EV fast-charging models and introduce a data-driven approach with an optimization model for deploying EV fast-chargers for both electric vehicles and heavy trucks traveling through a network of suburban highways. This deployment aims at satisfying EV charging demands while respecting the limits imposed by the electric grid. We also consider the availability of local photovoltaic (PV) farm and integrate its produced power to the proposed charging network. Finally, through a case study on Paris-Saclay area, we provide locations for EV charging stations and analyze the benefits of integrating PV power at different prices, production costs and charging capacities. The obtained results also suggest potential enhancements to the charging network in order to accommodate the increasing charging demand for EVs in the future.

Keywords: electric vehicles; charging; optimization; mobility; electric grid; territory; PV energy

Citation: Mourad, A.; Hennebel, M.; Amrani, A.; Hamida, A.B. Analyzing the Fast-Charging Potential for Electric Vehicles with Local Photovoltaic Power Production in French Suburban Highway Network. *Energies* **2021**, *14*, 2428. https://doi.org/10.3390/en14092428

Academic Editor: Javier Contreras

Received: 26 March 2021
Accepted: 20 April 2021
Published: 24 April 2021

1. Introduction

Electric vehicles (EVs) have witnessed a quickening development in recent years [1]. By improving their battery capacities and recharging technologies, EVs can circulate for long distances and be recharged in short periods of time (e.g., a Tesla Roadster can travel up to 340 km while recharging its battery takes no more than 20 min using fast-charging technology [2]). This development is also accompanied by some challenges, since it can reshape the future of electric mobility and affect people's lives on both social and economic levels [3]. These challenges include: the efficient distribution of charging facilities; the need for new legislative proposals to accelerate EVs integration to mobility systems; the development of efficient frameworks for modeling and calculating EV energy consumption and measuring their potential impacts on existing electric grids [4]; and the availability of optimized operational plans that can guarantee the quality of provided services and comply to people's needs [5].

With the increasing interest in using EVs in future transportation systems, the need for deploying fast-charging infrastructures, especially on highways and high-speed roads, becomes essential. To fulfill this need and determine its required investments, it is important to anticipate EV future charging demands and requirements and optimize their facility location taking into account the different mobility flows (i.e., small vehicles, heavy trucks, etc.) and the existing electric grid [6]. In addition, integrating new sources of renewable energy (e.g., photovoltaic power) into power systems represents one promising opportunity to fulfill the increasing demand for energy related to EV charging. Together,

vehicle electrification and renewable energy generation can help in providing a sustainable transportation service while reducing emissions of the road transportation sector [7].

In this paper, we start by providing a comprehensive classification of the related literature and its different models and solution approaches. Then, we develop a data-driven modeling approach along with an optimization model to solve the problem of positioning fast charging stations for EVs on a highway network. The proposed model takes into account EV charging demands based on the different mobility flows, including those for small vehicles and heavy trucks, as well as the constraints imposed by the available electric grid. In addition, the model considers the availability of a local photovoltaic farm and integrates its generated power to the grid to supply EV charging. More precisely, the deployment of EV charging stations and the number of fast-chargers is based on the charging demand in the first place. Then, this deployment must respect the restrictions of the electric grid as well as the availability of parking places at charging stations. For this purpose, we provide a mathematical formulation for the problem aiming at maximizing the covered charging demand (i.e., for both small electric vehicles and heavy trucks) while respecting investment budget limits and the available capacities provided by the electric grid. The underlying optimization problem corresponds to the well-known facility location problem where our facilities are the charging stations [8]. Through a case study on Paris-Saclay area, we provide locations for deploying EV charging stations as well as the number of fast chargers to be installed at each charging station. We also analyze the benefits of PV power integration and its productions costs and different charging capacities.

The paper is organized as follows. In Section 2, we provide a thorough classification of related literature. In Section 3, we describe the considered problem. The proposed modeling approach is then presented in Section 4. In Section 5, we present the computational study we have conducted. Finally, in Section 6, the key findings are highlighted and research perspectives are suggested.

2. Literature Review

Research on locating EV charging stations can be classified into three main categories: *transportation-based*, *electric-based* and *hybrid approaches* [9]. ***Transportation-based*** approaches focus on the transportation perspective when designing EV charging networks (i.e., mobility flows and passengers demand), while ignoring power system constraints [10]. Their main drawback is that they need to be readjusted according to the existing power system conditions. On the other hand, ***electric-based*** approaches aim to locate EV charging stations in power systems such that their capacity and security requirements are satisfied and the investment costs needed to upgrade them are minimized [11] (i.e., transportation constraints are ignored). These approaches also need to be readjusted according to the existing mobility conditions. Since both transportation and electric perspectives are important in our case, we develop a ***hybrid*** approach in this paper, where both types of constraints are considered [12]. We thus propose to deploy EV charging stations while taking into account both the actual transportation and power system conditions in the studied area.

From a transportation perspective, according to Zhang [13], there are three main planning methodologies for locating EV charging stations: *nodal demand-based*, *simulation-based* and *traffic flow-based* planning. In ***nodal demand-based*** planning, charging stations are located to satisfy EV charging demands that appear at some geographical locations. The main drawback is that some transportation network issues (e.g., traffic congestion) are ignored in this methodology. On the other hand, ***simulation-based*** and ***traffic flow-based*** planning estimate EV charging demands based on real-life transportation surveys and origin-destination traffic flow (OD matrices), respectively. However, simulating EV charging demands is computationally expensive, while EV driving-range limit is not often considered when planning traffic flow-based methods. Relatively, EV charging demands can be represented in different ways [9]. In ***point-based*** representations, EV charging demands are concentrated at certain points. In addition, ***polygon-based*** representations consider dividing the studied area into smaller sub-areas (e.g., polygons) where each

charging demand is represented by the centroid of the sub-area where it is located. The spatial attributes of the demand are thus ignored. Unlike the first two cases, ***network-based*** representations do not only consider the spatial attributes of the demand; they also reflect the existing highway network as well as the different travel patterns of travelers in the studied area (commute, transit, etc.). In this latter case, charging demands can appear during long-distance or short-distance trips (referred to as ***inter-city*** and ***intra-city***, respectively). As such, we use a traffic flow-based methodology in order to estimate EV charging demands where a network-based approach is used to represent them. This choice is made as it complies with our problem description and takes into account the availability of traffic flow data for the studied area.

From an electric perspective, different types of chargers have been considered in the literature: ***Level 1 chargers*** (referred to as *slow-charging*, 110V/15A), ***Level 2 chargers*** (220V/15-30A) and ***Level 3 chargers*** (referred to as *fast-charging*, 400-500V/50A) (Table 1). These chargers have different features and requirements, such as power capacities, charging times, cabling and outlets, etc. Some studies considered only one type of chargers, while other studies integrated different types of chargers into their models. For example, in [9], the distribution of *Level 2* charging stations among territory segments is considered, based on the potential use of EVs and the different parking behaviors. In [12], the focus is on selecting locations for fast-charging stations (*Level 3*) through a highway network for long-distance trips in the US. On the other hand, in [6], the deployment of both *Level 2* and *Level 3* chargers is considered to fulfil EV charging requirements while respecting the specifications of the electric grid. In this paper, we consider the deployment of *Level 3* chargers as the aim is to satisfy charging demands on a highway network where EVs need to be recharged at short charging times.

Table 1. Charging levels for EVs.

Chrg. Level	Input V/A	Max. Power	Chrg. Time
Level 1	120VAC-20A (16A usable)	1.92 kW (1-phase)	10–13 h
Level 2	400VAC-80A (64A usable)	25.6 kW (3-phase)	1–3 h
Level 3	600VAC-200A (160A usable)	96 kW (3-phase)	0.2–0.58 h

Many decision models have been proposed in the literature for modeling the problem of deploying EV charging stations. These models represent the mathematical formulation used to model the underlying operational problem. For example, some studies suggested to use a ***Facility Location Model (FLM)*** [9] or a ***set-covering*** model [14], while others introduced a ***Flow Refueling Location Model (FRLM)*** or one of its variants (e.g., *Multi-period FRLM*, *Capacitated FRLM*, etc.) as they provide a better coverage of mobility flows [10]. These different formulations share many features and constraints but can also vary depending on the problem setting and its application context. Different objectives can be assigned to these models, such as ***minimizing investment costs*** [15], ***maximizing covered mobility flows*** or ***the number recharged EVs*** [6] and ***minimizing*** CO_2 ***emissions*** [16]. The choice of which objective to use depends on the optimization problem itself and its overall aim.

Regarding modeling approaches, some studies assumed charging demands to be aggregated at certain nodes and aim to cover these demands by locating charging stations within a feasible distance or travel time of these nodes (***node-based modeling***) (e.g., EV charging demand in residential areas) [17]. Some other studies located charging demands through arcs linking different nodes (***arc-based modeling***) (e.g., charging demand through a highway linking two residential areas) [10]. Furthermore, more researchers are recently interested in modeling charging demands using sequences of nodes and arcs (***path-based modeling***) [18]. This combined approach has the advantage of modeling traffic flows where the aim is to locate charging stations so that the captured flow is maximized. In this paper, we consider a *facility location model (FLM)* where a path-based modeling approach is used in order to maximize the charging demand covered by the proposed network of fast-charging stations. Once the decision model is built, most studies suggested solving it using a ***mathe-***

matical solver (e.g., *Cplex*, *Gurobi* or other solvers) so that the optimal deployment of EV charging stations can be found. However, due to the potential complexity of the underlying optimization problem, some studies developed more sophisticated methods for solving these models, such as ***Branch-and-Bound (B&B)*** [13], ***Dynamic Programming (DA)*** [15] and ***Genetic Algorithms (GA)*** [14]. In this paper, we provide a data-driven framework in which we solve the proposed model using *Cplex* mathematical solver and analyze the obtained results. This is due to the limited number of variables in our model which allows finding solutions in feasible computational times (Section 4). Solving such models requires input data regarding different mobility and electric aspects. These datasets can either be based on real-life case studies (***real datasets***, as in our case) or on datasets that are generated randomly or using a simulation approach (***simulated datasets***). A comprehensive summary of the reviewed literature is presented in Table 2.

Finally, many recent studies focus on using green energy sources for supplying EV charging networks. In [19], a review of photovoltaic energy systems along with their sizing strategies, optimization techniques and cost evaluation methodologies is provided. In addition, the main indices for analyzing energy costs and pricing schemes is presented. A relevant application of these indices can be found in [20], where the investment of a photovoltaic energy system was evaluated through a case study in three different cities in Turkey. To model production uncertainty in photovoltaic energy systems, a scenario-based approach to evaluate the potential use of photovoltaic energy for charging EVs was introduced by Good [21]. The results of testing the proposed approach on two Scandinavian cities demonstrate that PV energy yield can cover EV demands in most of the considered scenarios. The necessity of stochastic approaches to deal with uncertainty in PV production was also confirmed by Thomas [22]. This was done by evaluating a set of case studies using a linear programming framework that takes into account PV uncertainty and stochastic EV driving schedules. In this paper, we consider the availability of local photovoltaic (PV) power station, study the use of its produced energy for supplying EV chargers and analyze their potential benefits as well as its different prices and production costs.

Table 2. Literature classification.

Reference	Discipline	Modeling Appr.	Planning Appr.	Model	Pattern	Demand Repr.	Objective	EV Charger	Solution Appr.	Data
Acha [17]	hybrid	node-based	demand	TCOPF	intra-city	point	min. cost	L2	CPLEX	simulated
Xi [23]	hybrid	node-based	flow	FLM	inter-city	polygon	max. EV charged	L1 and L2	CPLEX	simulated
Capar [10]	transport	arc-based	flow	FRLM	both	polygon	max. flow covered	NA	CPLEX	simulated
MirHassani [18]	hybrid	path-based	flow	FRLM	intra-city	network	min. cost	NA	CPLEX	simulated
Chung [24]	hybrid	path-based	flow	M-FRLM	inter-city	network	max. flow covered	L3	B&B CPLEX	real
Riemann [25]	hybrid	node-based	flow	FRLM	intra-city	point	max. flow covered	L2	CPLEX	simulated
Huang [26]	hybrid	node-based	demand	FC-GS	both	polygon	min. cost	L2 and L3	CPLEX	real
Guo [11]	hybrid	node-based	flow	MOPEC	intra-city	network	max. benefit	L3	Gurobi	simulated
Efthymiou [27]	transport	node-based	demand	NA	intra-city	point	min. No. of chargers	NA	GA	real
Yi [15]	hybrid	path-based	demand	FLM	intra-city	point	min. cost	L2 and L3	DA CPLEX	real
Sun [6]	hybrid	path-based	flow	FLM	intra-city	point	max. flow covered	L2 and L3	CPLEX	real
He [28]	hybrid	path-based	flow	FRLM	intra-city	network	max. flow covered	L2 and L3	CPLEX	simulated
Zhang [13]	hybrid	node-based	simulation	CFRLM	inter-city	point	min. cost	L3	B&B CPLEX	simulated
Liu [16]	hybrid	node-based	demand	FLM	intra-city	network	min. emissions	L2	PSOL	real
He [12]	hybrid	path-based	flow	FRLM	inter-city	network	max. EV charged	L3	MATLAB	real
Csiszar [9]	hybrid	node-based	simulation	FLM	inter-city	polygon	max. flow covered	L2	Bi-level CSL	real
Chen [29]	transport	node-based	demand	FLM	inter-city	point	min. cost	L2	Bi-level CSL	simulated
Vazifeh [14]	transport	node-based	demand	set-covering	intra-city	polygon	min. No. of stations	L2	Genetic algo.	real
Our paper	hybrid	path-based	flow	FLP	both	network	max. flow covered	L3	CPLEX	real

3. Problem Description

We introduce the considered operational problem and the modeling approach used to solve it using Paris-Saclay area as our case study. Paris-Saclay is an agglomeration community located at the south of Paris. As it is geographically close to the capital and to main economical activities, Paris-Saclay is traversed by many major mobility axes (e.g., A6, A10 and N20 in Figure 1). These axes are used by personal vehicles and heavy trucks for short-distance trips (e.g., commuting) as well as international transit flows. In addition, a large photovoltaic (PV) farm is to be installed at Marcoussis district (next to the intersection of "A10" and "N104" highways, Figure 1) with 76,500 PV panels and up to 24 GWh annual power production. The PV power will be raised to the voltage of the electric grid so that it can be injected into the distribution network. Thus, this farm has the potential of increasing charging power at nearby EV charging stations while reducing their reliance on the existing distribution network.

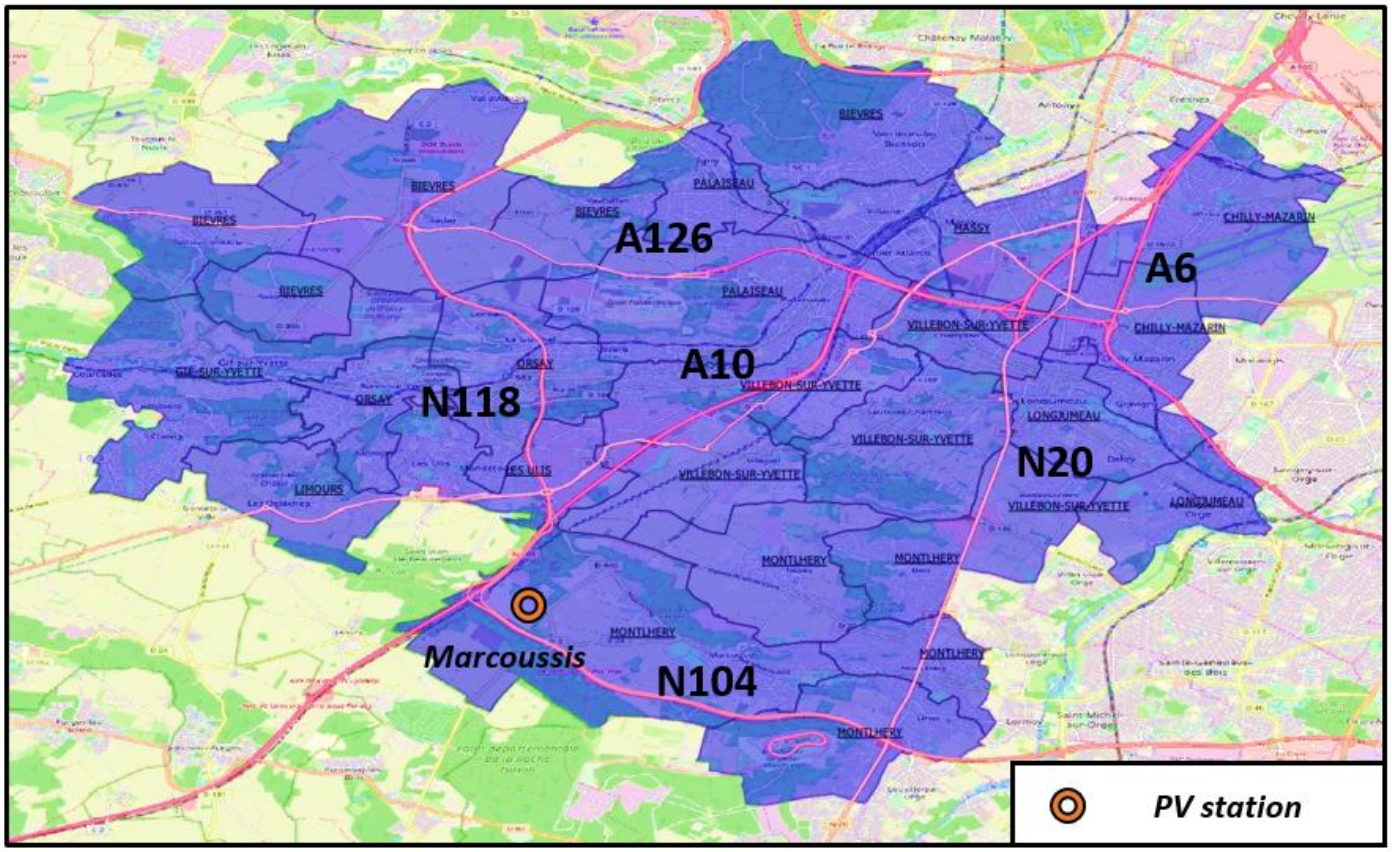

Figure 1. Paris-Saclay—major axes.

Based on these specifications, we provide a formal definition for the problem of locating EV fast-charging stations at Paris-Saclay area. First, we consider two types of fast chargers, one for charging small electric vehicles and the other for charging heavy electric trucks. In addition, We consider a set of potential charging locations $\mathcal{S} = \mathcal{I} \cup \mathcal{V}$, where $\mathcal{I}$ includes locations that are powered by the distribution network and $\mathcal{V}$ includes those that are powered by a local PV station. Every charging location $s \in \mathcal{S}$ is defined by a cost (c_s) indicating required investment to use this location as a charging station, and it has a maximum electric capacity and a max/min number of fast chargers that can be installed for small vehicles as well as heavy trucks (max_s^a, min_s^a, max_s^b and min_s^b, respectively). The investment cost (c_s) includes land cost (i.e., the cost required for purchasing the land where charging stations are to be installed) and cabling expenses (i.e., the extra expenses required to establish charging stations and connect them to the grid). For charging locations that are

powered by the distribution network, the maximum electric capacity is fixed and depends on the distribution network itself. We refer to this fixed capacity as q_s ($\forall\ s \in \mathcal{I}$). On the other hand, this capacity cannot be fixed for charging locations that are powered by PV energy as it highly depends on PV energy production which is stochastic (i.e., it depends on cloudiness index, season and solar irradiation). We thus refer to this varying electric capacity as λ_s ($\forall\ s \in \mathcal{V}$). To build mobility paths, we consider a set of coupling nodes N representing different highway intersections. As such, we consider a set of paths $\mathcal{P}$ that link sequences of coupling nodes. Every path $p \in \mathcal{P}$ is defined by its charging demands d_p^a and d_p^b, representing the number of electric vehicles and trucks, respectively, to be recharged per day. The set of charging locations that are associated with each path p is denoted as S_p. The numbers of electric vehicles and trucks that can be recharged using a fast charger per day are defined as β^a and β^b respectively. Similarly, the amounts of electric power needed to recharge an electric vehicle or an electric truck using a fast charger are defined as q^a and q^b respectively. Moreover, installing a fast charger for electric vehicles or trucks implies extra costs (i.e., charger costs). These costs are defined as c^a and c^b, respectively. For the sake of simplicity, we assume all electric vehicles to be homogeneous, and, thus, their recharging time and energy are the same. We consider the same assumption for electric trucks (notations and variables are summarized in Table 3).

Table 3. Notations and variables.

Indices:	
$\mathcal{S}$	Set of potential charging locations.
$\mathcal{I}$	Set of charging locations powered by distribution network.
$\mathcal{V}$	Set of charging locations powered by local PV station.
$\mathcal{N}$	Set of coupling nodes.
$\mathcal{P}$	Set of mobility paths.
$\mathcal{S}_p$	Set of charging locations associated with path p.
Parameters:	
β^a, β^b	Number of vehicles and trucks that can be recharged by a charger per day respectively.
q^a, q^b	Electric power needed to recharge a vehicle and a truck respectively.
c^a, c^b	Cost of installing a charger for vehicles and trucks respectively.
For every charging location $s \in \mathcal{S}$:	
c_s	Investment required to use location s as a charging station.
q_s, λ_s	Maximum electric capacity at location $s \in \mathcal{I}$ and $\mathcal{V}$ respectively.
min_s^a, max_s^a	Min. and max. number of vehicle chargers that can be installed at location s.
min_s^b, max_s^b	Min. and max. number of truck chargers that can be installed at location s.
For every path $p \in \mathcal{P}$:	
d_p^a	Charging demand for vehicles at path p.
d_p^b	Charging demand for trucks at path p.
Decision variables:	
$x_s =$	$\begin{cases} 1 & \text{if a charging station is deployed at location } s \\ 0 & \text{otherwise} \end{cases}$
y_p	Demand coverage rate at path p, $y_p \in [0, 1]$.
z_a^s	Number of vehicle chargers to be installed at location s.
z_b^s	Number of truck chargers to be installed at location s.

Hence, the choice of deploying a charging station at location $s \in \mathcal{S}$ and the number of fast chargers to be installed is based on the recharging demand through the path where s is located. However, the number of chargers to be installed is limited by the available electric capacity and the availability of places and parking slots at location s. As such, we build a model to optimize this deployment by maximizing the satisfied demand while respecting the different constraints.

4. Modeling Framework

We introduce our data-driven modeling framework using Paris-Saclay area as a case study. This framework consists of three stages: (i) modeling EV charging demand and network (Section 4.1); (ii) modeling PV power production and analyzing its different scenarios (Section 4.2); and (iii) providing an optimization model to find the final distribution of EV fast-chargers (Section 4.3).

4.1. Modeling Demand and Charging Network

To build the charging network and its associated demand, we start by defining a set of coupling nodes. For this purpose, we consider the intersections of major axes to be the set of coupling nodes (Figure 2). This is because mobility flows usually change after an intersection where new vehicles can join or leave the different flows. We thus define 17 coupling nodes $n_1, n_2, \ldots, n_{17}$ covering the highway network at Paris-Saclay (Figure 2a).

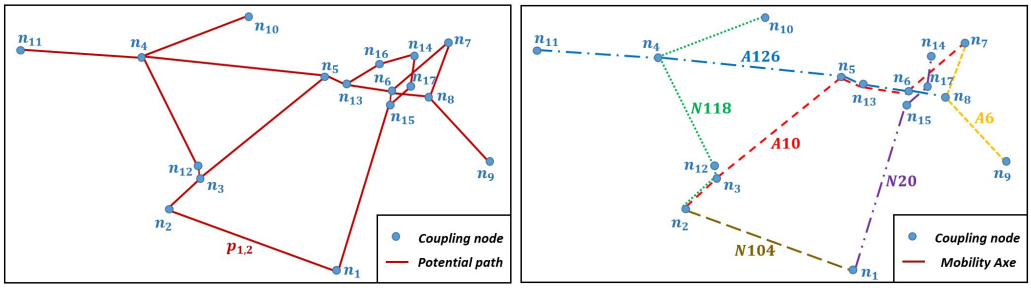

(**a**) Coupling nodes (**b**) Mobility axes

Figure 2. Modeling mobility paths.

Mobility paths are then constructed using sequences of these nodes. For example, a potential path "N20" is defined by the sequence of nodes (n_1, n_{15}, n_{17} and n_{14}) (Figure 2b). However, we need to consider the actual mobility flows (i.e., the actual number of vehicles traveling at each potential path) in order to define paths more precisely. We therefor consider the flow records provided by DiRIF (Road Direction in Ile-de-France region). Based on traffic counters located at different points in Paris-Saclay area, these records indicate the number of vehicles and heavy trucks traversing each road segment on hourly and daily basis. These records are thus used to define paths with homogeneous EV flows. If we take the "N20" example, we observe that its mobility flow changes after crossing coupling node n_{15}. This is due to other, relatively smaller, departmental roads that intersect with it at this point. Another example can be found at the road segment linking nodes n_2 and n_3 where both "A10" and "N118" highways overlap (Figure 2b). Traffic flow is combined at this segment and thus need to be considered separately of the rest of the flow on both highways. Following the same reasoning, we define nine different paths based on the actual mobility flows at Paris-Saclay area (Table 4). Each path is associated with vehicle and truck flows and their charging demands.

In addition, we consider the actual EV charging stations proposed by the Paris-Saclay Agglomeration Community (CPS). Some of these stations are currently operational and some are projected over the next few years (Figure 3). The choice of considering these stations can be justified by the fact that their locations are already considered to be suitable by the local authorities. However, not all these locations are suitable for our case. This is because many of them require long detours by EVs traveling on highways in order to be accessed. Another reason is that not all these stations are intended for domestic or commercial charging (i.e., *Level 2* and *Level 3* chargers), and, thus, not designed to accommodate EV fast-charger (e.g., electric and spacing restrictions). As such, we filter this initial set of potential charging locations and we select those that are located at feasible distances from major axes (e.g., $\leq$10 km) where the installation of *Level 3* chargers is possible for both vehicles and trucks.

Table 4. Defined mobility paths.

Path	Axes	*n* Nodes	*s* Nodes
p_1	A10	n_3, n_5	s_0, s_{11}, s_{91}
p_2	A10, A126	n_5, n_{13}, n_6, n_7	s_{58}, s_{18}, s_{51}, s_{93}, s_{87}, s_{95}
p_3	A6	n_9, n_8, n_7	s_{23}, s_{48}
p_4	N118, A10	n_2, n_3, n_{12}	s_{81}
p_5	N118	n_{12}, n_4, n_{10}	s_{94}, s_{88}, s_{62}, s_{13}, s_{28}, s_{84}
p_6	A126	n_{11}, n_4, n_5, n_8	s_{35}, s_{79}, s_3, s_{77}, s_{33}
p_7	N20	n_1, n_{15}	s_{25}, s_{89}, s_{90}, s_{86}
p_8	N20	n_{15}, n_{17}, n_{14}	s_{83}, s_{92}
p_9	N104	n_1, n_2	s_{96}, s_{97}

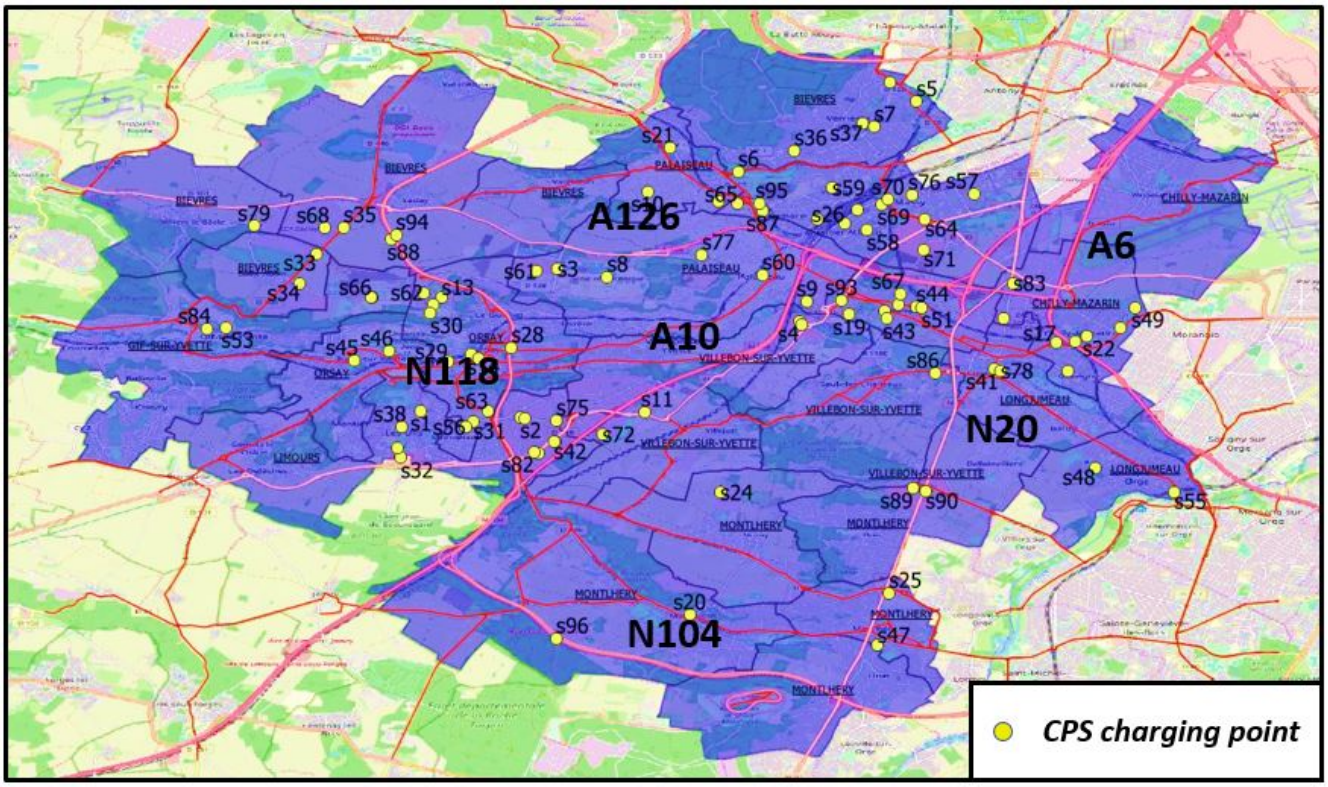

Figure 3. EV charging network-CPS charging points.

We also consider the actual service stations that are located on highways in order to enhance the charging network. This is because service stations can be among the first to adapt fast-charging facilities as soon as EV charging demand increases. The final set of potential charging locations is then selected based on the initial set of CPS charging locations and the set of highway service stations at Paris-Saclay (Figure 4). These potential locations are powered by the distribution network. Costs, electric grid specifications and the maximum number of fast chargers that can be installed at each location are fixed based on their real data (data of charging stations, land costs and electric network specifications are provided by Paris-Saclay Agglomeration Community (CPS)). Charging locations are then associated to paths so that the model can decide which locations to use and how many chargers to install at each location (see Figure 5 for an overview of considered paths and their potential charging locations).

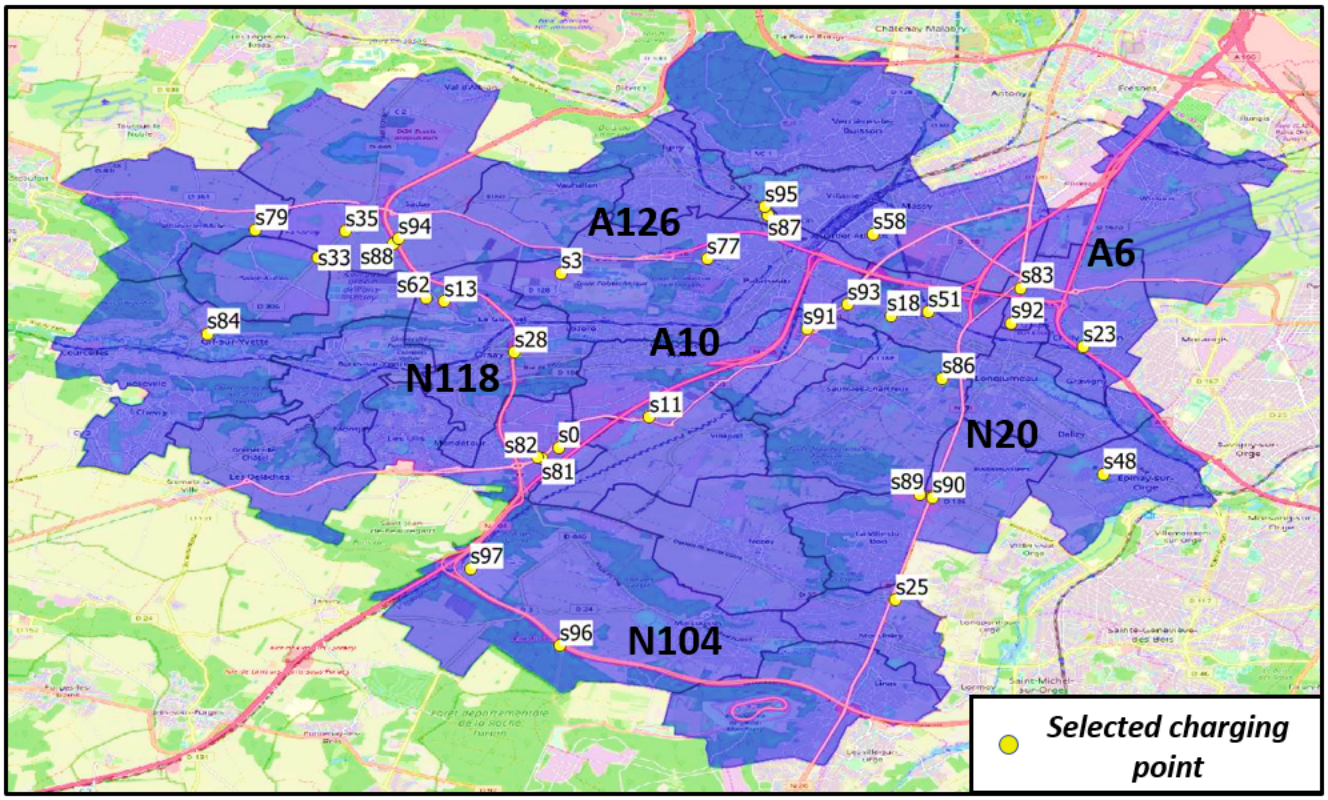

Figure 4. EV charging network: Selected charging points.

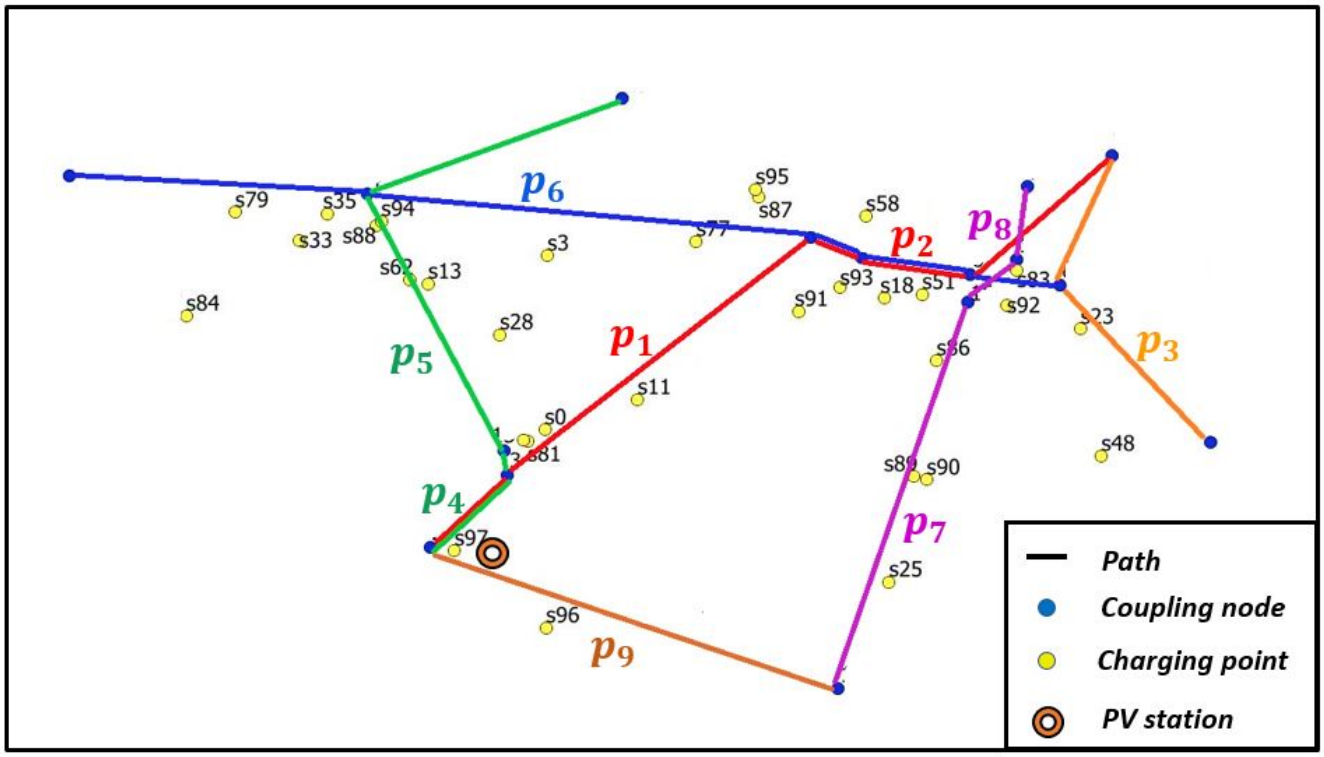

Figure 5. Paris-Saclay: Mobility paths and charging points.

4.2. Modeling PV Power Production

As introduced above, we consider the availability of a photovoltaic farm that can be integrated to the charging network (Figure 5). Unlike power provided by the distribution

grid, PV power production is stochastic as it depends on varying factors. According to Diop [30], the generated power of a PV farm at instant t can be calculated as follows:

$$P(t) = (1 - \mu(t)) \times I(t) \times \delta \times \eta \quad (1)$$

where $\mu(t)$ is the cloudiness index at instant t (%), $I(t)$ is the irradiation at instant t (W/m^2), δ is the surface of PV panels (m^2) and η is the efficiency that corresponds to the electric quantity produced as a percentage of the received PV power. We assume that this power is used for charging EVs. This generated power highly depends on irradiation and cloudiness index as they differ during seasons and day hours. For example, PV production is maximal in a sunny day during Summer at noon. The actual values of irradiation at different seasons and day hours are fixed, and thus known in advance (we use data provided by the Photovoltaic Geographical Information System (PVGIS) to build the irradiation matrix for Paris-Saclay area). Based on real irradiation values, we estimate the amount of PV energy that can be produced by the considered PV farm during a sunny day at each month of the year (Figure 6). We observe that up to 90 MWh/day can be generated during summer months when irradiation is at its highest, while this production drops to approximately 30 MW/day during winter. However, these values can be seen as the maximal daily production (i.e., calculated in fully-sunny days), and thus will be reduced due to cloudiness effects.

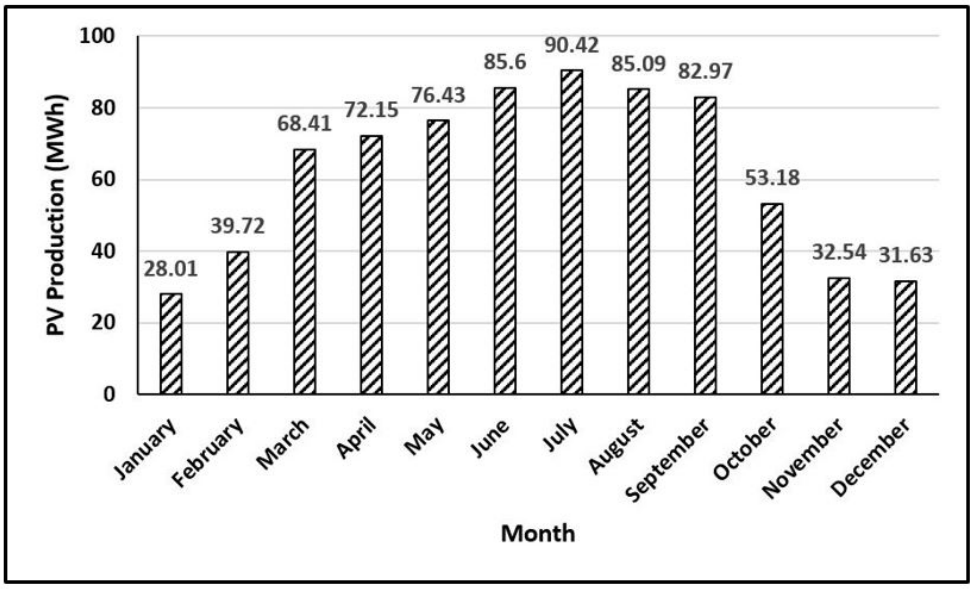

Figure 6. Maximal daily PV production per month.

Unlike the irradiation, the cloudiness index ($\mu(t)$) cannot be fixed in advance as it depends on weather conditions (i.e., $\mu(t)$ is stochastic). We thus need to model this uncertainty using a set of scenarios and calculate their probability distribution. We consider four different day profiles:

- *Fully-Sunny* (where $\mu(t)$ is between 0% and 25%)
- *Partially-Cloudy* (where $\mu(t)$ is between 25% and 50%)
- *Mostly-Cloudy* (where $\mu(t)$ is between 50% and 75%)
- *Fully-Cloudy* (where $\mu(t)$ is between 75% and 100%)

In addition, we divide the day into eight time periods (i.e., (12AM,3AM), (3AM,6AM), .. , (9PM,12AM)). These day periods help in capturing different mobility patterns (e.g., period (6AM-9AM) is a peak period when people commute, etc.). We also consider the four seasons (e.g., the probability of having a fully-sunny day is higher in summer than in winter, Table 5). As a result, we build our set of scenarios, where every scenario is defined by a *day-profile*, a *day-period* and a *season* (i.e., 128 different scenarios in total). To calculate

their probabilities, we use weather measurements of the last 10 years and we cluster them according to day profiles, periods and seasons using K-Means approach [22] (weather data for Paris-Orly airport, including cloudiness index, are provided by Météo France). We chose K-Means clustering as it classifies weather measurements into clusters with the nearest mean. An initial set of four cluster centres was selected. The four clusters for each time step (day-period abd season) represent four possible scenarios for the cloudiness index $\mu(t)$ (i.e., fully-sunny, partially-cloudy, mostly-cloudy and fully-cloudy). Weather measurements for each time step are thus assigned to one of the four clusters with the closest centroid. Centroid values are then updated by calculating the average of the objects population in each cluster. The discrete probability for each scenario is then calculated based on the population of objects allocated to each cluster (i.e., centroid) for every time step resulting in a probability matrix. The resulting probability matrix is then used by our optimization model to anticipate the amount of power that can be generated by the PV farm at the different scenarios.

Table 5. Cloudiness index-Paris Orly (2010–2020).

	Winter	**Spring**	**Summer**	**Autumn**
Fully-Sunny	16.9%	27.2%	35.6%	22.9%
Partially-Cloudy	6.7%	9.1%	15.6%	9.1%
Mostly-Cloudy	11.4%	17.6%	21.5%	11.6%
Fully-Cloudy	65.1%	46.1%	27.3%	56.2%

4.3. Mathematical Modeling

To formulate the optimization model, we introduce a binary variable x_s, which is equal to 1 if a charging station is deployed at location $s \in \mathcal{S}$ and 0 otherwise. In addition, we introduce a continuous variable $y_p \in [0,1]$ representing the demand coverage rate on path p and two integer variables, z_s^a and z_s^b, representing the number of fast chargers to be installed at charging location $s \in \mathcal{S}$ for electric vehicles and trucks, respectively. The optimization model is thus formulated as follows:

$$Max\ Z = \sum_{p \in \mathcal{P}} (d_p^a + d_p^b)\, y_p \tag{2}$$

s.t.

$$\sum_{s \in \mathcal{S}} c_s x_s + c^a z_s^a + c^b z_s^b \leq \mathcal{C} \tag{3}$$

$$\sum_{p \in \mathcal{P}} (d_p^a + d_p^b)\, y_p \geq \mathcal{Q} \tag{4}$$

$$\sum_{s \in \mathcal{S}_p} \beta^a z_s^a \geq d_p^a \qquad \forall\, p \in \mathcal{P} \tag{5}$$

$$\sum_{s \in \mathcal{S}_p} \beta^b z_s^b \geq d_p^b \qquad \forall\, p \in \mathcal{P} \tag{6}$$

$$min_s^a \leq z_s^a \leq max_s^a \qquad \forall\, s \in \mathcal{S} \tag{7}$$

$$min_s^b \leq z_s^b \leq max_s^b \qquad \forall\, s \in \mathcal{S} \tag{8}$$

$$q^a z_s^a + q^b z_s^b \leq q_s \qquad \forall\, s \in \mathcal{I} \tag{9}$$

$$q^a z_s^a + q^b z_s^b \leq \lambda_s \qquad \forall\, s \in \mathcal{V} \tag{10}$$

$$if\ y_p = 0 \implies z_s^a + z_s^b = 0 \qquad \forall\, s \in \mathcal{S}_p,\ \forall\, p \in \mathcal{P} \tag{11}$$

$$if\ z_s^a + z_s^b > 0 \implies x_s = 1 \qquad \forall\, s \in \mathcal{S} \tag{12}$$

$$x_s \in \{0,1\},\ y_p \in [0,1] \qquad \forall\, s \in \mathcal{S},\ \forall\, p \in \mathcal{P} \tag{13}$$

$$z_s^a,\ z_s^b,\ q_s,\ \lambda_s,\ \in \mathcal{N} \qquad \forall\, s \in \mathcal{S} \tag{14}$$

$$d_p^a,\ d_p^b,\ \beta^a,\ \beta^b,\ q^a,\ q^b\ \in \mathcal{N} \qquad \forall\, p \in \mathcal{P} \tag{15}$$

$$min_s^a,\ max_s^a,\ min_s^b,\ max_s^b\ \in \mathcal{N} \qquad \forall\, s \in \mathcal{S} \tag{16}$$

$$c_s,\ c^a,\ c^b\ \in \mathcal{R} \qquad \forall\, s \in \mathcal{S} \tag{17}$$

The objective function (2) aims at maximizing the total covered demand for charging both vehicles and trucks. Regarding model constraints, constraint (3) ensures that the sum of location costs and chargers installation costs does not exceed total budget limit of the project. Constraint (4) states that a minimum coverage of the overall charging demand must be ensured (e.g., at least 30% of the overall demand must be covered). Constraints (5) and (6) ensure that charging demands, for vehicles and trucks respectively, are covered by the proposed charging stations at each mobility path. Constraints (7) and (8) state that the number of fast chargers to be installed must respect the specified limits at each charging location. These limits are defined using space constraints at each location (i.e., number of possible parking slots). Constraint (9) ensures that the electric power required to operate the installed chargers at a specific charging location does not exceed the available electric capacity provided by the distribution network at that location. Similarly, constraint (10) ensures that the electric power needed at charging locations, where a PV station is located nearby, must not exceed the actual PV energy production provided by that station. Constraints (11) and (12) are used to link the different variables of the model and ensure the coherence of their values. Finally, constraints (13)–(17) define domains for the introduced variables and parameters.

Note that constraints (11) and (12) are formulated as implications, and thus need to be linearized. Using standard linearization techniques, we express them by one or two linear inequalities as follows:

$$z_s^a + z_s^b + My_p \leq M \qquad \forall\, s \in \mathcal{S}_p,\ \forall\, p \in \mathcal{P} \tag{18}$$

$$z_s^a + z_s^b - My_p \leq -M \qquad \forall\, s \in \mathcal{S}_p,\ \forall\, p \in \mathcal{P} \tag{19}$$

$$x_s - M(z_s^a + z_s^b) > -M \qquad \forall\, s \in \mathcal{S} \tag{20}$$

where (18) and (19) are the linearizations of constraint (11), (20) is the linearization of constraints (12) and M is a big integer number.

5. Results and Discussion

In this section, we present the results of our case study including the proposed deployment of fast-chargers with different levels of EV charging demand (Section 5.1). We then analyze the benefits of PV power integration in different scenarios and varying charging capacities (Section 5.2). Finally, we study the different energy prices and production costs and we analyze their impact on the profitability of the project (Section 5.3).

5.1. Deploying EV Fast-Chargers

We tested the proposed model using Paris-Saclay data in order to obtain the complete deployment of EV charging stations in the area. The different elements of the model were implemented in Python 2.7.8. CPLEX 12.6.3 solver was used for solving the optimization model. Instances of Paris-Saclay were tested on a core i7-8650U machine with 16 GB of RAM. Regarding test parameters, we assume that a fast charger requires 50 kW (≈20 min) for recharging an electric vehicle and 250 kW (≈30 min) for recharging an electric truck. This means that a fast charger can recharge up to 36 vehicles or 24 trucks per day. The costs of installing a fast charger for vehicles and trucks are estimated at 12 k€ and 15 k€, respectively (charger materials and installation costs are estimated based on their actual prices in the French market and adapted according to their equivalents in the international market KELWATT). The actual charging demand (i.e., the number of EVs to be recharged) was then calculated by considering 5% of the overall daily flow on each of the defined paths. This percentage is fixed based on EV sales share of the French automobile market in 2020 [31]. The model was also tested with higher rates as presented below in this section. Test parameters are summarized in Table 6.

Table 6. Test parameters.

Parameter	Value	Parameter	Value
c^a	12 k€	c^b	15 k€
β^a	36 vehicles	β^b	24 trucks
q^a	50 kW	q^b	250 kW

The obtained results indicate the number of chargers to be installed at each selected location (z_s^a and z_s^b in Figure 7). It can be observed that the number of vehicle chargers is relatively higher than that for trucks at all selected locations. This can be explained by the higher number of vehicles to be recharged at different paths. Another important observation is that the proposed deployment can cover up to 33.1% of the overall EV charging demand. More precisely, some paths are fully-covered (e.g., "A126" with 100%), some are partially-covered (e.g., "A10" and "N118" with 38% and 64%, respectively) and some others are poorly-covered (e.g., "A6" and "N104" with only 3.8% and 8.3%, respectively). Low coverage rates at some paths are due to the small number of charging locations and the limited electric capacity at these locations. It is also due to the relatively-high charging demand at these paths. To overcome this issue, new charging stations need to be installed and charging power and the grid capacity need to be increased at these poorly-covered paths.

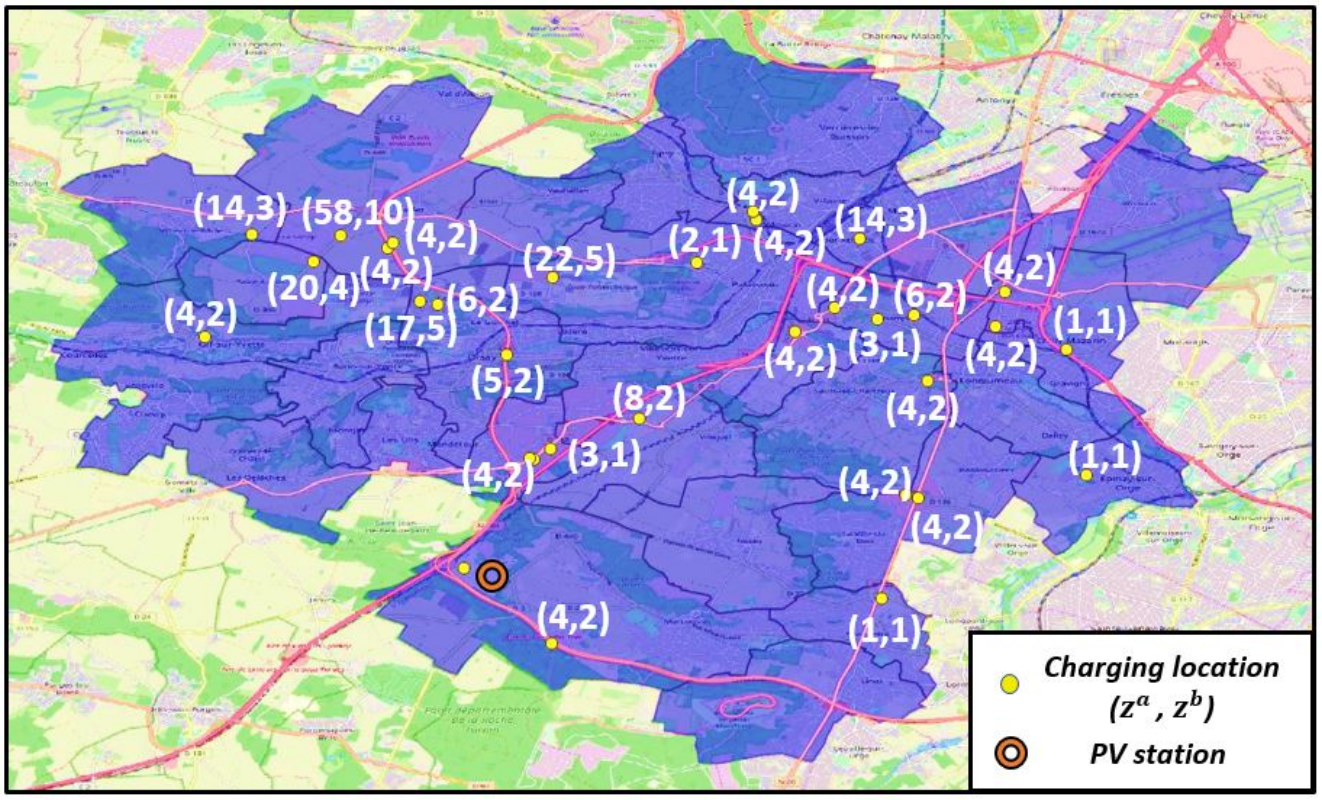

Figure 7. Number of chargers per station.

As mentioned above, we consider a charging demand that represents 5% of the overall flow which is partially-covered in proposed solution (33.1%). It is also considered that the number of chargers that can be installed is limited by the capacity of the electric grid and the availability of parking places at each location (constraints 7, 8, 9 and 10 in Section 4.3). We relax these constraints in the following in order to obtain a deployment that can fully satisfy higher rates of charging demand (i.e., 100% coverage rate). We thus increase the percentage of vehicles and trucks that need to be recharged and we observe the number of fast chargers needed to cover this increasing demand. In Table 7, the different rates of charging demand are given in the first column. The overall demand represented by the number of vehicles and trucks to be recharged is then given ("*Demand per hour*"). The number of fast chargers to be installed with their associated coverage rates and installation costs are indicated in columns "*No. of Chargers*", "*Covered*" and "*Cost (€)*", respectively. Compared to the original case (given in the first row in bold), we observe that satisfying full charging demands requires relatively increasing the number of chargers installed even when demand rate is conserved (i.e., 5%). With more EVs expected to circulate in the near future, satisfying higher rates of charging demand can become difficult as the number of chargers required along with their installation costs might not be affordable due to economic and logistics reasons (10% and 20% rates in Table 7). These observations also justify the need to enhance the capacity of the electric grid (e.g., PV power integration) to accommodate this increase. In addition, new advances in fast-charging technology can help in reducing EV charging times, thus requiring fewer chargers in the network. Although all EVs might not need to be partially or fully charged in the considered area, these observations can help in anticipating the future needs of EV charging which include improving the existing charging facilities, installing new ones or suggesting improvements to the electric grid. As such, this analysis can be further enhanced by taking into account the variable charging EV demands during day hours. Analyzing this variability can be essential in determining the required enhancements to both the charging network and the electric grid. However, this requires extending the proposed approach by developing a

simulation framework in order to anticipate this variable demand at different mobility patterns and day hours (commuting, morning and evening flows, weekend flows, etc.).

Table 7. Cost and demand coverage with different EV rates .

Rate	Demand per Hour		No. of Chargers		Covered	Cost (€)	Extra (€)
	No. of Vehicles	No. of Trucks	Vehicle	Truck			
5%	**1985**	**218**	**255**	**72**	**31.1%**	**4032K**	**-**
5%	1985	218	683	111	100%	9753 K	5721 K
10%	3970	436	1456	218	100%	19,914 K	15,882 K
20%	7940	872	2650	436	100%	38,380 K	34,348 K

5.2. Analyzing PV Power Integration

The considered PV farm is located at the intersection of "A10" and "N104" which are poorly-covered paths (Figure 7). Thus, integrating its produced energy has the potential of enhancing the coverage rates at these paths as more chargers can be installed. To analyze this potential benefit, we quantify the amount of energy that can be produced at different scenarios and we calculate the demand coverage rate at each case. We then compare the obtained rates to the case where no PV production is considered (Table 8). By averaging 10 different runs of the model, we observe that coverage rates can increase from 3.8% and 8.3% to 47.1% and 74.2%m respectively during summer where PV production is maximal. This positive impact can also be witnessed on the overall coverage rate with approximately 7–11% increase in spring and summer scenarios. As a result, locally-produced PV energy can help in enhancing the quality of EV charging service especially along paths where the demand is high and electric grid capacity is limited. The proposed approach can thus be extended in order to accommodate other PV farms that can be installed at the area. This potential can be higher if these farms are to be installed at paths where EV charging demands are high (e.g., next to A6 highway).

Table 8. Demand coverage with PV production per season.

	No PV	PV-Wint.	PV-Spr.	PV-Sum.	PV-Aut.
Overall	33.1%	37.3%	40.9%	44.4%	39.1%
A10	3.8%	19.9%	33.5%	47.1%	27.1%
N104	8.3%	29.9%	53.3%	74.2%	39.8%

Furthermore, we tested the proposed model with different charging powers. We thus increased the charging power of chargers by up to 1.5, 2 and 4 times and analyzed its impact on covered charging demand. Increasing charging power of chargers can be similar to increasing the number of chargers from energy consumption and charging time perspectives. However, using two chargers requires higher installation and land cost as we need two parking places, where we only need one parking place in the case of using one, more powerful, charger. We observe that, as chargers become more powerful, the demand coverage percentage increases (up to 40.9%, 52.5% and 71.1%, respectively, Figure 8). This also highlights the importance of increasing the capacity of these chargers and integrating new PV farms to accommodate this increase. However, it is important to mention that PV farms rely on their annual energy production more than power peaks and profiles throughout a day or a season. A high power consumption (charging) combined with a high PV energy production can thus create flow fluctuations to the grid unless they are well synchronized. In addition, connecting PV farms to the electric grid means that charging EVs can heavily rely on the grid in winter months when PV power production is not sufficient [32]. This issue opens the door for using other renewable sources, such as wind turbines and geothermal power plants, in order to decrease the reliance on the electric grid during winter. Although injecting multiple renewable energy sources to the electric

grid can provide many benefits, it can also lead to increased financial expenses. As such, more research is being directed towards developing new hybrid systems where different renewable sources of energy are integrated to the grid. Such systems aim at providing well-optimized solutions in terms of both energy and expenses so that customer demands are satisfied at feasible production costs.

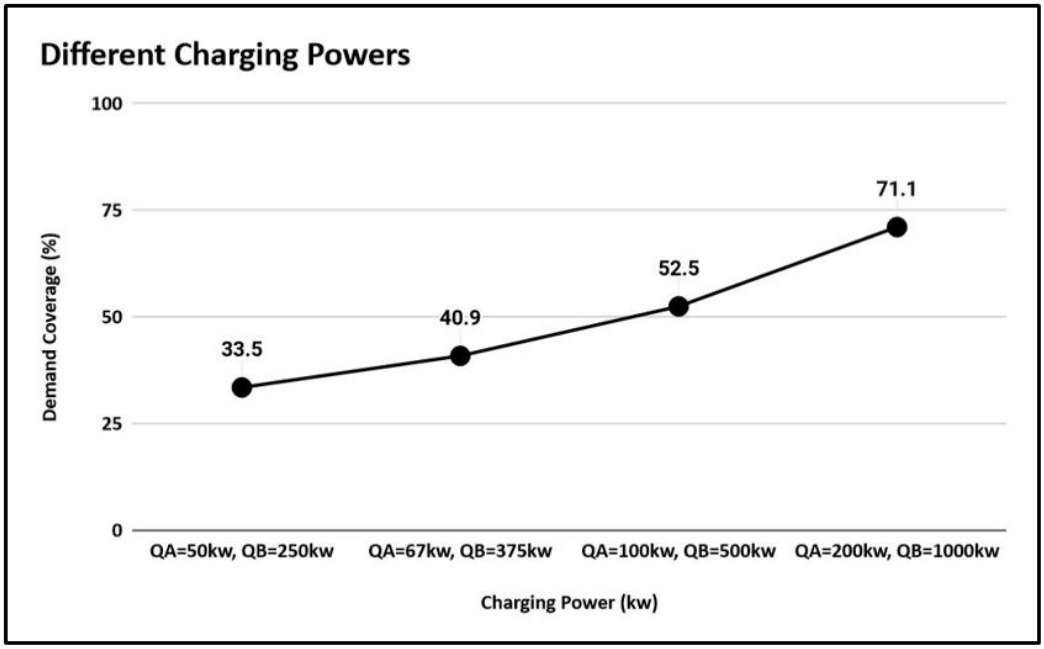

Figure 8. Demand coverage with different charging powers.

5.3. Analyzing Energy Prices and Production Costs

We studied three different investment indices to evaluate the profitability of integrating PV energy. First, *Levelized Cost of Energy (LCOE)* represents the average net cost of electricity generation for the planned PV farm over its lifetime [19]. It can be calculated as the ratio between lifetime costs and energy production, as follows:

$$LCOE = \frac{\sum_{t=1}^{n} \frac{I_t + M_t + F_t}{(1+r)^t}}{\sum_{t=1}^{n} \frac{E_t}{(1+r)^t}} \quad (21)$$

where I_t, M_t and F_t are the investment, maintenance and fuel costs in year t, E_t is the electricity generation in year t and r is the discount rate. Second, *Return on Investment (ROI)* is used to evaluate the efficiency of an investment by measuring its amount of return [20]. It is calculated by dividing project net income to its total cost, as follows:

$$ROI = \frac{Project\ return\ (income - cost)}{Project\ cost} \times 100 \quad (22)$$

Third, *Payback Period (PP)* represents the amount of time needed to recover the cost of an investment. It can be calculated by dividing overall project investment to its annual profit, as follows:

$$PP = \frac{Investment\ amount}{Annual\ profit} \quad (23)$$

The project of installing the PV farm at Paris-Saclay area requires an investment of 20 M€. The investment costs (I_t) appear only in the first year as they represent the cost

of installing PV panels and EV fast-chargers (estimated at 870 K€ based on the number of chargers proposed by the model, c^a and c^b in Table 6). Maintenance costs (M_t) of a PV farm appear every three years and are estimated at 10% of the annual profit (National Center of Photovoltaic Resources (CRPV)). Fuel costs (F_t) are ignored in this case and the annual electricity generation (E_t) is estimated at 24 GWh (i.e., we assume that all generated PV power is used for charging EVs). Discount rate (r) is fixed at 5%. In addition, project income is the difference between PV production cost (i.e., the calculated *LCOE*) and the price of selling this energy for charging EVs. In France, the price of charging an EV using a Tesla super-charger is 0.2 €/kWh. This price includes the cost of installing Tesla fast chargers as well. Thus, the cost of generating a kilowatt at the PV farm (including the cost of installing EV chargers) must be less than 0.2 € in order to have a positive income.

PV farms are often evaluated over a 20-year lifetime [20]. However, we calculated the introduced indices on 10-, 15- and 20-year lifetimes (Table 9). The results show that net cost of the generated PV energy (*LCOE*) is estimated at 0.11, 0.08 and 0.07 €/kWh over different lifetime intervals. These values can be seen as the minimum cost required for selling electricity at break-even prices so that project expenses can be recovered during its lifetime. Relatively, the planned investment brings a positive return of 260% over a 20-year lifetime. This means that every 100 € of investment in the considered PV farm will be returned as 260 € at the end of its lifetime. These positive *ROI* values justify the benefits of using the locally-produced PV energy for supplying EV chargers. Regarding the refund time of investment (*PP*), the results indicate the considered investment will be able to pay itself back in approximately seven years, which is less than half of the project lifetime.

Table 9. PV energy-Cost analysis.

	10 Years	15 Years	20 Years
Levelized Cost of Energy (LCOE)	0.11	0.08	0.07
Return on Investment (ROI)	148%	224%	260%
Payback Period (PP)	9.66	7.39	6.65

6. Conclusions

In this paper, a data-driven approach and an optimization model for the deployment of EV charging stations through a network of highways is introduced. The model was tested using a Cplex solver and a case study on Paris-Saclay area was performed. After selecting optimal locations for charging stations, the results highlight the benefits of integrating PV energy production on improving demand coverage rates. In addition, the economical benefits of this integration were quantified ($ROI = 260\%$ over 20 years lifetime).

The main perspectives of this research can be summarized in two levels. On the methodological level, the proposed approach can be extended to consider multiple renewable energy sources and integrate their power to the electric grid. Another interesting research direction is to consider EV battery states and the possibility of storing energy excess at charging stations during low-demand periods, so that it can be used later to charge EV at high-demand periods. This can lead to more realistic scenarios as both EV charging demand and PV production vary in different seasons and hours of the day. In addition, a stochastic programming approach can be developed for modeling uncertainty in PV production and better estimating its different scenarios. On the analytical level, besides analyzing the benefits of using PV energy for charging EVs, it is also important to study the impacts of this integration on the electric grid in terms of its infrastructure, as well as its effects on other sources of electric demands (e.g., transport, domestic, commerce, etc.). Finally, anticipating future charging demands and capacities represents a key passage for improving the obtained solution and adapting it to the future needs of EV charging networks. We thus believe that this study helps in better understanding the potential deployment of EV fast-charging stations in real-life applications and, thus, promoting more research towards studying this rising trend in the future.

Author Contributions: Conceptualization, M.H. and A.B.H.; methodology, A.M. and M.H.; software, A.M.; validation, M.H., A.A. and A.B.H.; formal analysis, all authors; data curation, A.M.; writing—original draft preparation, A.M.; writing—review and editing, M.H., A.A. and A.B.H.; supervision, M.H.; project administration, M.H. and A.B.H.; and funding acquisition, M.H. and A.B.H. All authors have read and agreed to the published version of the manuscript.

Funding: This research received no external funding.

Acknowledgments: This research work was carried out as part of the PGMO research project at GeePs laboratory within CentraleSupélec engineering school. The work is also in collaboration with the Institute of Research and Technology SystemX (IRT-SystemX) and the Agglomeration Community of Paris-Saclay (CPS).

Conflicts of Interest: The authors declare no conflict of interest.

References

1. Mourad, A.; Puchinger, J.; Chu, C. A survey of models and algorithms for optimizing shared mobility. *Transp. Res. Part B Methodol.* **2019**, *123*, 323–346. [CrossRef]
2. Shareef, H.; Mainul Islam, M.D.; Mohamed, A. A review of the stage-of-the-art charging technologies, placement methodologies, and impacts of electric vehicles. *Renew. Sustain. Energy Rev.* **2016**, *64*, 403–420. [CrossRef]
3. Macioszek, E. E-mobility infrastructure in the Górnoslasko—Zaglebiowska Metropolis, Poland, and potential for development. In Proceedings of the World Congress on New Technologies, Lisbon, Portugal, 18–20 August 2019.
4. Madhusudhanan, A.K.; Na, X.; Cebon, D. A Computationally Efficient Framework for Modelling Energy Consumption of ICE and Electric Vehicles. *Energies* **2021**, *14*, 2031. [CrossRef]
5. Jones, C.B.; Lave, M.; Vining, W.; Garcia, B.M. Uncontrolled Electric Vehicle Charging Impacts on Distribution Electric Power Systems with Primarily Residential, Commercial or Industrial Loads. *Energies* **2021**, *14*, 1688. [CrossRef]
6. Sun, Z.; Gao, W.; Li, B.; Wang, L. Locating charging stations for electric vehicles. *Transp. Policy* **2018**, *98*, 48–54. [CrossRef]
7. Fachrizal, R.; Shepero, M.; van der Meer, D.; Munkhammar, J.; Widén, J. Smart charging of electric vehicles considering photovoltaic power production and electricity consumption: A review. *eTransportation* **2020**, *4*, 100056. [CrossRef]
8. Deb, S.; Tammi, K.; Kalita, K.; Mahanta, P. Review of recent trends in charging infrastructure planning for electric vehicles. *Wiley Interdiscip. Rev. Energy Environ.* **2018**, *7*, e306. [CrossRef]
9. Csiszár, C.; Csonka, B.; Földes, D.; Wirth, E.; Lovas, T. Urban public charging station locating method for electric vehicles based on land use approach. *J. Transp. Geogr.* **2019**, *74*, 173–180. [CrossRef]
10. Capar, I.; Kuby, M.; Leon, V.; Tsai, Y. An arc cover–path-cover formulation and strategic analysis of alternative-fuel station locations. *Eur. J. Oper. Res.* **2013**, *227*, 142–151. [CrossRef]
11. Guo, Z.; Deride, J.; Fan, Y. Infrastructure planning for fast charging stations in a competitive market. *Transp. Res. Part C Emerg. Technol.* **2016**, *68*, 215–227. [CrossRef]
12. He, Y.; Kockelman, K.M.; Perrine, K.A. A Optimal locations of U.S. fast charging stations for long-distance trip completion by battery electric vehicles. *J. Clean. Prod.* **2019**, *214*, 252–461. [CrossRef]
13. Zhang, H.; Moura, S.J.; Hu, Z.; Song, Y. PEV Fast-Charging Station Siting and Sizing on Coupled Transportation and Power Networks. *IEEE Trans. Smart Grid* **2018**, *9*, 2595–2605. [CrossRef]
14. Vazifeh, M.M.; Zhang, H.; Santi, P.; Ratti, C. Optimizing the deployment of electric vehicle charging stations using pervasive mobility data. *Transp. Res. Part A Policy Pract.* **2019**, *121*, 75–91. [CrossRef]
15. Yi, Z.; Shirk, M. Data-driven optimal charging decision making for connected and automated electric vehicles: A personal usage scenario. *Transp. Res. Part C Emerg. Technol.* **2018**, *86*, 37–58. [CrossRef]
16. Liu, Q.; Liu, J.; Le, W.; Guo, Z.; He, Z. Data-driven intelligent location of public charging stations for electric vehicles. *J. Clean. Prod.* **2019**, *232*, 531–541. [CrossRef]
17. Acha, S.; van Dam, K.H.; Shah, N. Modelling spatial and temporal agent travel patterns for optimal charging of electric vehicles in low carbon networks. In Proceedings of the 2012 IEEE Power and Energy Society General Meeting, San Diego, CA, USA, 22–26 July 2012; IEEE: New York, NY, USA, 2012; pp. 1–8.
18. MirHassani, S.A.; Ebrazi, R. A Flexible Reformulation of the Refueling Station Location Problem. *Transp. Sci.* **2013**, *47*, 617–628. [CrossRef]
19. Khan, F.A.; Pal, N.; Saeed, S.H. Review of solar photovoltaic and wind hybrid energy systems for sizing strategies optimization techniques and cost analysis methodologies. *Renew. Sustain. Energy Rev.* **2018**, *92*, 937–947. [CrossRef]
20. Ozcan, O.; Ersoz, F. Project and cost-based evaluation of solar energy performance in three different geographical regions of Turkey: Investment analysis application. *Eng. Sci. Technol. Int. J.* **2019**, *22*, 1098–1106. [CrossRef]
21. Good, C.; Shepero, M.; Munkhammar, J.; Boström, T. Scenario-based modelling of the potential for solar energy charging of electric vehicles in two Scandinavian cities. *Energy* **2019**, *168*, 111–125. [CrossRef]

22. Thomas, D.; Deblecker, O.; Ioakimidis, C.S. Optimal operation of an energy management system for a grid-connected smart building considering photovoltaics' uncertainty and stochastic electric vehicles' driving schedule. *Appl. Energy* **2018**, *210*, 1188–1206. [CrossRef]
23. Xi, X.; Sioshansi, R.; Marano, V. Simulation–optimization model for location of a public electric vehicle charging infrastructure. *Transp. Res. Part D Transp. Environ.* **2013**, *22*, 60–69. [CrossRef]
24. Chung, S.H.; Kwon, C. Multi-period planning for electric car charging station locations: A case of Korean Expressways. *Eur. J. Oper. Res.* **2015**, *242*, 677–687. [CrossRef]
25. Riemann, R.; Wang, D.Z.W.; Busch, F. Optimal location of wireless charging facilities for electric vehicles: Flow-capturing location model with stochastic user equilibrium. *Transp. Res. Part C Emerg. Technol.* **2015**, *58*, 1–12. [CrossRef]
26. Huang, K.; Kanaroglou, P.; Zhang, X. The design of electric vehicle charging network. *Transp. Res. Part D Transp. Environ.* **2016**, *49*, 1–17. [CrossRef]
27. Efthymiou, D.; Chrysostomou, K.; Morfoulaki, M.; Aifantopoulou, G. Electric vehicles charging infrastructure location: A genetic algorithm approach. *Eur. Transp. Res. Rev.* **2017**, *9*, 27. [CrossRef]
28. He, J.; Yang, H.; Tang, T.Q.; Huang, H.J. An optimal charging station location model with the consideration of electric vehicle's driving range. *Transp. Res. Part C Emerg. Technol.* **2018**, *86*, 641–654. [CrossRef]
29. Chen, R.; Qian, X.; Miao, L.; Ukkusuri, S.V. Optimal charging facility location and capacity for electric vehicles considering route choice and charging time equilibrium. *Comput. Oper. Res.* **2020**, *113*, 104776. [CrossRef]
30. Diop, F. *Probabilistic Load Flow Computation for Unbalanced Distribution Grids with Distributed Generation*; Paris-Saclay University: Gif-sur-Yvette, France, 2018.
31. Funke, S.Á; Sprei, F.; Gnann, T.; Plötz, P. How much charging infrastructure do electric vehicles need? A review of the evidence and international comparison. *Transp. Res. Part D Transp. Environ.* **2019**, *77*, 224–242. [CrossRef]
32. Vlad, C.; Bancila, M.A.; Munteanu, T.; Murariu, G. Using renewable energy sources for electric vehicles charging. In Proceedings of the 2013 4th International Symposium on Electrical and Electronics Engineering (ISEEE), Galati, Romania, 11–13 October 2013; pp. 1–6.